Comparative Study of Radiative Flux from Mushroom BLEVE Model

Anas Mbarki, Aziz Ettahir, and Abderraouf Guelzim

Nomenclature

V_{FB}	The total volume of the fireball (m^3)
V_{S}	Spherical volume (m^3)
V_{C}	Cylindrical volume (m^3)
FL	Filing level of the vessel
t_{d}	The fireball duration (s)
t_{lo}	The fireball Liftoff Time (s)
$D_{\max}$	Maximum fireball diameter (m)
D_{FB}	The fireball diameter (m)
r_{FB}	The fireball radius (m)
H_{FB}	The height of the center of the fireball (m)
r_{S}	The radius of the spherical part of the mushroom (m)
r_{C}	The radius of the disk of the cylindrical part of the mushroom (m)
h_{C}	The height of the cylindrical part of the mushroom (m)
$m_{\mathrm{t_{lo}}}$	The mass of fuel involved on the liftoff time (kg)
ρ	The density (kg/ m^3)
α	The coefficient of proportionality or the volume ratio
L_*	The linear scale length
U_*	The linear scale velocity (the characteristic velocity owing to the buoyancy force) (m/s)
t_*	The linear scale time
V_*	Characteristic volume

A. Mbarki (✉) · A. Ettahir
Materials, Energy and Acoustics Team (MEAT), Mohammed V University in Rabat—EST Salé, Rabat, Morocco
e-mail: anas_mbarki@um5.ac.ma

A. Guelzim
Forensic Institute of the Royal Gendarmerie, Rabat, Morocco

R. K Agarwal (ed.), *Recent Advances in Manufacturing Engineering and Processes*, Lecture Notes in Mechanical Engineering,
https://doi.org/10.1007/978-981-19-6841-9_14

ΔHc	Heat of combustion (kJ/kg)
M_0	Mass of fuel involved (kg)
ρ_a	The density of ambient air density (kg/ m^3)
$c_{p,a}$	The specific heat capacity of air (kJ/kg)
T_a	The temperature of ambient air (K)
a	Constant
Fr	The Froude number
U_0	The release velocity (m/s)
g	Acceleration due to gravity (m/s)
X	The distance (m)
F_{FB}	The max geometric view factor for a spherical emitter (−)
C_{max}	The max geometric view factor for a cylindrical emitter (−)
C_V	The vertical view factor for a cylindrical emitter (−)
C_h	The horizontal view factor for a cylindrical emitter (−)
q	The radiative flux (kW/m^2)
E_s	The emissive power of fire per unit surface area (W/m^2)
f_h	The radiative fraction of the heat of combustion (−)
M	The initial mass of fuel in the fireball (mass) (kg)
τ_an	The atmospheric transmissivity (−)
R	The fractional relative humidity
Pv	The saturated vapor pressure of water at the ambient temperature (Pa)

1 Introduction

The prevention of risks associated with major industrial accidents is a necessity for those responsible for site safety management. Since the slightest error in estimating its dangers may have disastrous consequences on both people and structures, hence the need to set up efficient and valid analytical models for estimating the effects of these phenomena. This study is an attempt to model the thermal effects of a Bleve, taking into consideration the numerous hazards that can influence this phenomenon, namely the time and the distance from the source of the radiation, and finally the behavior of the flaming gas cloud facing the upward entrainment of ambient air. The mushroom Bleve model can be an alternative, making it possible to take into account all its hazards by containing them in a single model, which varies throughout the combustion duration.

2 Methods

During failure or total rupture of a storage tank for flammable chemicals or hydrocarbons, the increased difference in the pressure of the products contained and the ambient pressure favors the evaporation the liquid almost instantaneously; the spread evaporated liquid forms a cloud which gradually grows following the entrainment of the ambient air toward the interior of the cloud. The operation accentuated by the phenomena of turbulence and ascending velocity, as observed in different experiments, gives a shape resembling mushroom to the fireball in the phase of volume growth. These phenomena are not taken into account by the dynamic model which claims that the shape of the cloud is almost spherical and that only its size varies with time.

In this work, we calculate the radiative flux from a proposed mathematical model, and then compare it with that obtained by using the dynamic forecasting model, which assumes the fireball to have a spherical geometry. This proposed mathematical model is applied to a reservoir with a total volume of 10,796 m^3, with a filling level of 40%, under a pressure of 15 bars, and then compared to Martinsen and Marx's dynamic model (Martinsen et al. 1999; INERIS 2017; Johnson and Pritchard 1990; https://www.aiche.org/resources/publications/books/guidelines-consequence-analysis-chemical-releases).

3 Discussion of Results

3.1 The Real Fireball Geometry: "Mushroom Shape"

The model of fireball's mushroom shape behavior is similar to the one described by the following figure (Fig. 1); the total volume V_{FB} is composed of a spherical volume and a cylindrical volume denoted, respectively V_S and V_C.

So, we have:

$$V_{FB} = V_S + V_C \tag{1}$$

Fig. 1 Mushroom Bleve volume

The volumes of the geometric shapes (spherical and cylindrical) obtained are proportional to the volume of the initial fireball, considering that:

$$V_C = \alpha \cdot V_{FB}. \tag{2}$$

$$V_S = (1 - \alpha) \cdot V_{FB} \tag{3}$$

where α: is a dimensionless constant between 0 and 1, it is introduced to express the proportionality between the volume of the sphere of the Martinsen and Marx model (Martinsen et al. 1999) and the volume of the spherical part of the considered mushroom geometry.

3.2 Modeling of the Mushroom Shape Approach

As observed in several accidents and confirmed in various recent experiments (British Gas experiments), the mushroom shape model illustrates a more realistic representation of the true behavior of fireballs. By employing adequate equations that take into account the fireball growth, the lift-off, the changing radiation characteristics, the visible cloud expansion velocity, the fuel properties (boiling temperature, heat of evaporation), the uplift velocity time scale of the fireball (Makhvilade et al. 1996, 1997, 1999a, 1999b, 2000; Makhviladze and Yakush 2005; Gostintsev 2022), the air entrainment as well as the turbulence associated to the ascendant air flux.

During the first third of Bleve's life, the analysis of the behavior associated with phenomenon's study is similar to that used in a dynamic model. The fireball has a spherical shape.

Thereafter, during the beginning of the second third of the burning time, the fireball stretches to take a new shape similar to that of a mushroom, formed by the superposition of two geometric shapes, a spherical part above the cylindrical part. The radius of this spherical part is less than that of the initial sphere; however, it always remains proportional to it.

3.3 Determination of the Volume's Characteristics Forming the Mushroom and of the Volume Ratio A

The radius, the height of the cylindrical part of the mushroom, and its radius are given by the following equations:

$$r_C = \frac{2}{3} \cdot \sqrt{\frac{\alpha}{t - \sqrt[3]{1-\alpha}\big/3}} \cdot r_{FB} \tag{4}$$

$$h_C = H_{FB} - r_S \tag{5}$$

$$r_S = \sqrt[3]{1-\alpha} \cdot r_{FB} \tag{6}$$

Determination of Alpha According to Makhviladze et al. (https://www.aiche.org/resources/publications/books/guidelines-consequence-analysis-chemical-releases; Makhvilade et al. 1996, 1997, 1999a), the characteristic volume V_* of the fireball is determined by equating the total combustion energy of the fuel $\Delta H_C M_0$ to the thermal energy of the cloud $\rho_b c_p (T_b - T_a) V_*$, where the subscript b corresponds to the combustion products.

And using the dimensionless analysis, for the linear scale length and the characteristic velocity owing to the buoyancy forces, we find:

$$V_* = \Delta H_c M_0 \big/ \rho_a c_{p,a} T_a \tag{7}$$

$$L_* = v_*^{1/3} \tag{8}$$

$$U_* = (L_* g)^{1/2} \tag{9}$$

Reducing the initial Eqs. (7–9), the Froude number which describes the buoyancy of the phenomenon can thus be expressed by:

$$\mathrm{Fr} = \left(\frac{U_0}{U_*}\right)^2 = \frac{U_0^2}{g}\left(\frac{\rho_a c_{p,a} T}{\Delta H_c M_a}\right)^{1/3} \tag{10}$$

After using the empirical relation which gives the maximum diameter of the fireball as the mass's function of the fuel entrained by ambient air:

$$D_{\max} = a \cdot M_0^{1/3} \tag{11}$$

Then, the explicit form of the dimensionless constant α is as follows:

$$\alpha = 1 - \left[\frac{1}{M_0} \cdot \left(U_0^2 \big/ a \cdot g\mathrm{Fr}\right)^3\right] \tag{12}$$

where α is the constant of the ratio between the maximum diameter of the fireball and the mass to the power 1/3.

3.4 Radiative Flux Measurement

The numerical values are calculated from the input data proposed in Sect. 2 methodology; the equations constituting the dynamic model are illustrated in (Eqs. 1–3).

First Step: 0 < t < t_d/3 We calculated the heat flux q at a certain distance from the fire experienced by the receiver per m^2, utilizing:

$$q = E_S \cdot F_{FB} \cdot \tau_a \tag{13}$$

$$E_s(t) = 0.0133 \cdot f_h \cdot H_c \cdot M^{12} \tag{14}$$

$$E_s(t) = 359.347, \text{ for} \rightarrow 0 \le t \le 2.127$$

$$F_{FB}(X, t) = D_{FB}(t)^2 \big/ 4 \cdot \left[H_{FB}(t)^2 + X^2\right] \tag{15}$$

$$F_{FB}(X, t) = \frac{\left(8.664 \cdot M^{1/4} t^{1/3}\right)^2}{4 \cdot \left[\left(4.332 \cdot M^{1/4} t^{1/3}\right)^2 + X^2\right]}$$

$$F_{FB}(X, t) = 3772.905 \cdot t^{2/3} \Big/ 4 \cdot \left(943.226 \cdot t^{2/3} + X^2\right)$$

$$\tau_a(x, t) = 2.02 \cdot \left\{\mathrm{RP_V}\left[\sqrt{H_{FB}(t)^2 + x^2} - \frac{D(t)}{2}\right]\right\}^{-0.09} \tag{16}$$

$$\tau_a(x, t) = 1.03 \cdot \left[\sqrt{943.226 \cdot t^{2/3} + X^2} - 30.712 \cdot t^{1/3}\right]^{-0.09}$$

Second Step: t_d/3 < t < t_d The radiative flux q at a certain distance from the fire experienced by the receiver, using:

$$q = q_{\text{spherical}} + q_{\text{cylindrical}} \tag{17}$$

$$q = E_S \cdot (F_{\text{spherical}} + F_{\text{cylindrical}}) \cdot \tau_a \tag{18}$$

$$E_s(t) = E_{\max} \cdot \frac{3}{2}\left(1 - \frac{t}{t_d}\right), \text{ for} \rightarrow \frac{1}{3} t_d < t \le t_d \tag{19}$$

$$E_{\mathrm{s}}(t) = 539 - 84.48 \cdot t, \text{ for} \rightarrow 2.127 < t \leq 6.381$$

$$\alpha = 1 - \left[\frac{1}{M_0} \cdot \left(U_0^2 \big/ a \cdot g\mathrm{Fr} \right)^3 \right] \tag{20}$$

$$\alpha = 34.25\% \approx 34\%$$

- $r_C = 0.381 \cdot \sqrt{\frac{1}{t-0.29}} \cdot r_{\mathrm{FB}}$

$$r_{\mathrm{C}} = 15.353 \Big/ \sqrt{t - 0.29}$$

- $h_{\mathrm{C}} = H_{\mathrm{FB}} - r_{\mathrm{S}} = 18.570 \cdot t - 34.388$
- $r_{\mathrm{S}} = 0.871 \cdot r_{\mathrm{FB}} = 34.388\,\mathrm{m}$

$$F_{\mathrm{Mushroom_{max}}} = F_{\mathrm{spherical}} + F_{\mathrm{cylindrical}} \tag{21}$$

$$F_{\mathrm{spherical}} = D_{\mathrm{S}}(t)^2 \big/ 4 \cdot \left[H_{\mathrm{FB}}(t)^2 + X^2 \right] \tag{22}$$

$$F_{\mathrm{spherical}} = 4730.103 \big/ 4 \cdot (344.852 \cdot t^2 + X^2)$$

$$F_{\mathrm{cylindrical}} = \sqrt{C_{\mathrm{H}}^2 + C_{\mathrm{V}}^2} \tag{23}$$

$$C_{\mathrm{H}} = \frac{1}{\pi} \cdot \left[\tan^{-1} \left(\frac{X + r_{\mathrm{C}}}{X - r_{\mathrm{C}}} \right)^{1/2} - \frac{X^2 - r_{\mathrm{C}}^2 + h_{\mathrm{C}}^2}{\sqrt{A \cdot B}} \cdot \tan^{-1} \left(\frac{(X - r_{\mathrm{C}}) \cdot A}{(X + r_{\mathrm{C}}) \cdot B} \right)^{1/2} \right] \tag{24}$$

$$C_{\mathrm{V}} = \frac{1}{\pi} \cdot \left[\frac{r_{\mathrm{C}}}{X} \tan^{-1} \left(\frac{h_{\mathrm{C}}^2}{X^2 - r_{\mathrm{C}}^2} \right)^{1/2} + \frac{h_{\mathrm{C}} \cdot (A - 2X \cdot r_{\mathrm{C}})}{X \cdot \sqrt{A \cdot B}} \tan^{-1} \left(\frac{(X - r_{\mathrm{C}}) \cdot A}{(X + r_{\mathrm{C}}) \cdot B} \right)^{1/2} - \frac{h_{\mathrm{C}}}{X} \tan^{-1} \left(\frac{X - r_{\mathrm{C}}}{X + r_{\mathrm{C}}} \right)^{1/2} \right] \tag{25}$$

With:

$$A = (X + r_{\mathrm{C}})^2 + h_{\mathrm{C}}^2 \tag{26}$$

$$B = (X - r_C)^2 + h_C^2 \tag{27}$$

$$\tau_a(X, t) = 2.02 \cdot \left\{ \mathrm{RP_V} \left[\sqrt{H_{FB}(t)^2 + X^2} - \frac{D_S(t)}{2} \right] \right\}^{-0.09} \tag{28}$$

$$\tau_a(X, t) = 1.03 \cdot \left[\sqrt{344.852 \cdot t^2 + X^2} - 17.194 * 2 \right]^{-0.09}$$

3.5 Graphic Comparison Between the Two Models

Figures 2, 3, 4, 5, and 6 are plots of the same data calculated by the mushroom approach compared to the measurements taken during British Gas test no. 4 and Martinsen and Marx model, at several distance. These plots give us an overview on the validity of the analytical predictions. who have been calculated from the mushroom Bleve model, compared to the analytical prediction of Martinsen and Marx model and to the measurements recorded during test no. 4 of the BG experience and this at several times during the combustion time, depending on the distance of the target from the tank. At the same time, it illustrates the variation of the incident thermal radiation received as a function of distance and as a function of time. The variation of the thermal radiation incident represented in Figs. 2, 3, 4, 5, and 6 shows a strong similarity to the trend and a strong positive correlation almost perfect to the results collected on the BG experiment no. 4.

The analysis of Fig. 7 gives us the following information:

The thermal dose of the spherical part during the last two thirds of the combustion time of the Bleve is equal to the area *s* (104.112). While the thermal dose of the cylindrical part during the same period of combustion of the Bleve is equal to the area *t* (45.76).

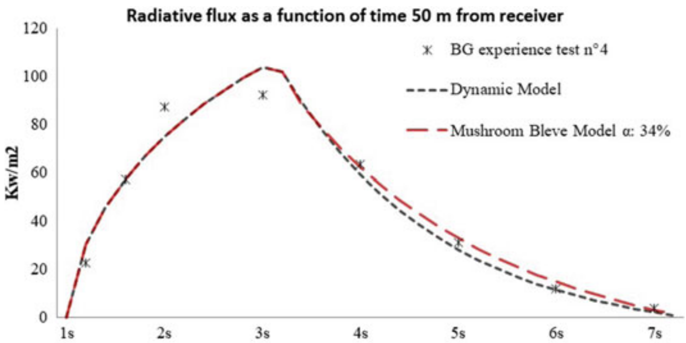

Fig. 2 Radiative flux as a function of time calculated at 50 m from receiver

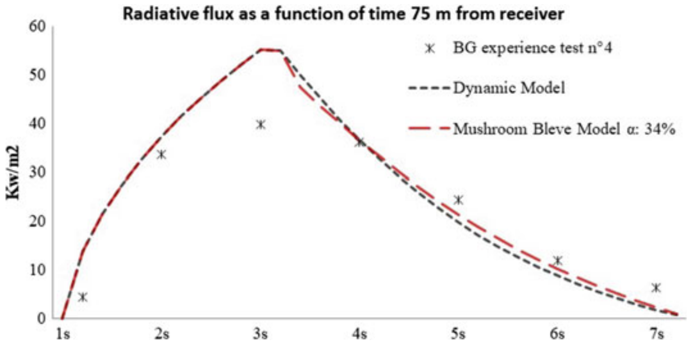

Fig. 3 Radiative flux as a function of time calculated at 75 m from receiver

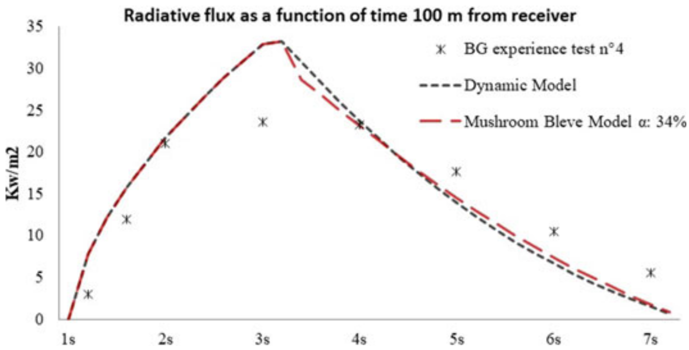

Fig. 4 Radiative flux as a function of time calculated at 100 m from receiver

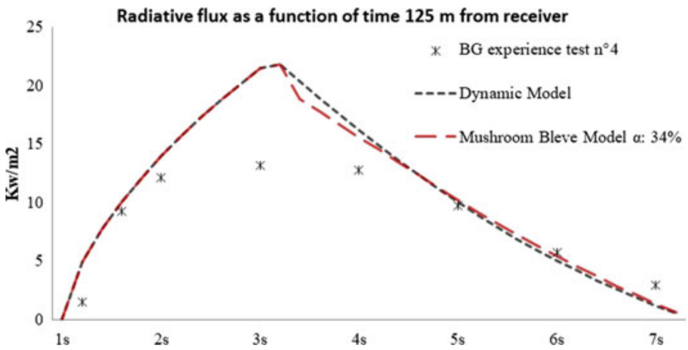

Fig. 5 Radiative flux as a function of time calculated at 125 m from receiver

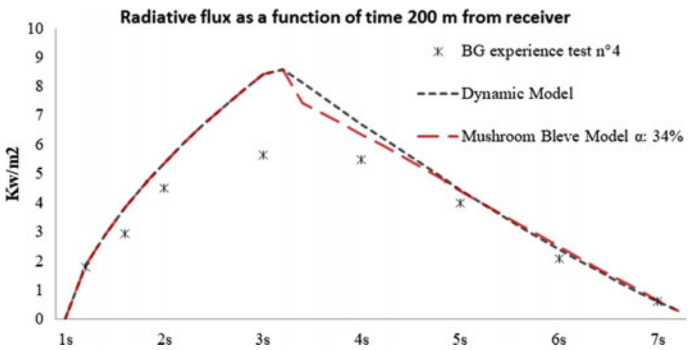

Fig. 6 Radiative flux as a function of time calculated at 200 m from receiver

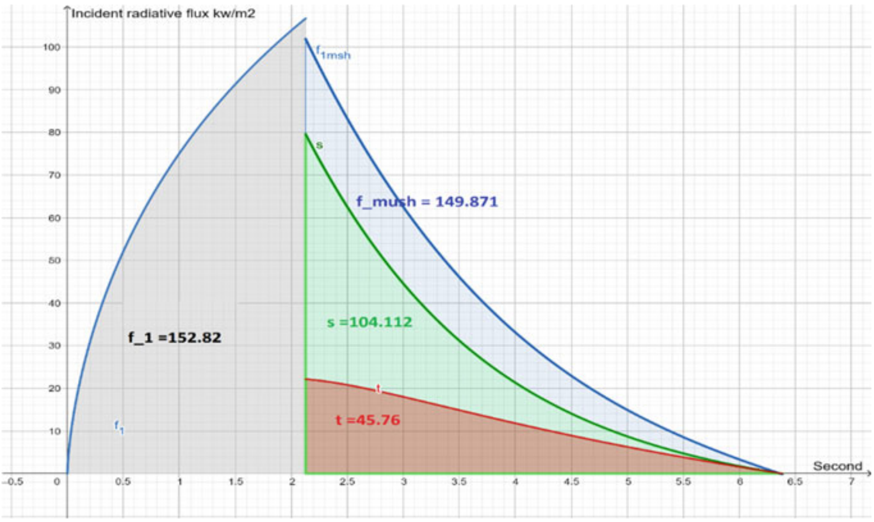

Fig. 7 Contribution of the cylindrical part of the Bleve mushroom in the calculation of the incident radiative flux at 50 m—measured during the simulation of BG test 4

The contribution of the cylindrical part is almost 30% of the thermal dose received by a target moving away from 50 m from the center of the phenomenon and this during the last two thirds of the combustion time of the Bleve, and more than 15% of the total thermal dose received by a target exposed to the incident radiative flux throughout the duration of the Bleve.

3.6 Discussion

The mushroom Bleve model has a great similarity with the dynamic model of Martinsen. It can be seen that, the radiative fluxes are calculated as a function of time and can be split into two parts:

- The first part at any instant t of the first third of the Bleve duration:

  The two models give the same values of the radiative flux.

- The second part at any instant t is greater than the first third:

  At the start of the second third, the radiative flux calculated by the dynamic model is greater than that calculated by the mushroom Bleve model, by few milliseconds for receivers located at a short or medium distance that does not exceed 100 m from the center of the geometric mushroom shape. In addition, the difference between the radiative fluxes calculated by the two models does not exceed 2.6 kw/m^2; this translates in a negative variance which does not exceed 6% for the radiative flux calculated by our approach. While this duration is extended to more than one second for receivers placed at a greater distance, and the difference between the radiative fluxes calculated by the two models does not exceed 1.6 kw/m^2, this is transcribed into a negative variance which does not exceed order of 7% for the radiative flux calculated by our approach.

  The ratio is quickly reversed, and the radiative flux calculated by the mushroom Bleve model takes values higher than that calculated by the dynamic model and this throughout the remaining existence time.

  For receivers located at a short or medium distance, which does not exceed 100 m from the center of the geometric mushroom shape, the difference between the radiative fluxes calculated by the two models does not exceed 5 kw/m^2; this translates into a positive variance which does not exceed 24% for the radiative flux calculated by our approach. While this variance does not exceed 1 kw/m^2, i.e., an increase of less than 5% of the radiative flux calculated by our approach. The magnitude of the calculation difference margin between the two models dissipates as the receiver moves away from the radiation source.

4 Conclusion

A In this study, two models relating to the effects of radiative transfers of a fireball generated by a Bleve were compared:

- Martinson and Marx's dynamic model, whose fireball geometry is considered to be spherical;
- Andour proposed model, whose fireball's geometry is considered to have a mushroom shape.

The comparison of the two models was made based to the experimental data for medium-scale fireball tests realized by Johnson and Pritchard (1990) as part of the experiments conducted by British Gaz and cited by INERIS (INERIS 2017).

The mushroom Bleve model is an attempt in which we made sure to take into account the real behavior of the fireball through the combustion duration following the analysis of the media library of the tests carried out, in order to define its temporal behavior.

This attempt will allow us to minimize the margin of error relating to the calculation of the thermal dose received by an individual relative to its distance from the radiation source. Thus, the effective distances and the impact on structure and people are expected to be more severe.

Although the difference is not appreciable in terms of safety, it takes into account the geometric reality of the Bleve phenomenon throughout its lifetime.

References

Gostintsev: Theory of the Aerodynamics, Autoignition. Google Scholar. https://scholar.google.com/scholar_lookup?title=Theory%20of%20the%20aerodynamics%2C%20self%20ignition%2C%20and%20burnup%20of%20turbulent%20thermals%2C%20vortex%20rings%2C%20and%20jets%20in%20a%20free%20atmosphere&journal=Khim.%20Fiz.&volume=9&pages=1279-1290&publication_year=1982&author=Gostintsev%2CYu.%20A.&author=Solodovnik%2CA.%20F.&author=Lazarev%2CV.%20V. Last accessed 2022 Feb 25

Guidelines for Consequence Analysis of Chemical Releases. https://www.aiche.org/resources/publications/books/guidelines-consequence-analysis-chemical-releases. Last accessed 2022 Feb 25

INERIS: OMEGA5 Le BLEVE, phénoménologie et modélisation des effets. INERIS, Verneuil-en-Halatte (2017)

Johnson, D., Pritchard, M.: Large scale experimental study of boiling liquid expanding vapour explosions (BLEVEs) (1990)

Makhvilade, G.M., Roberts, J.P., Yakush, S.E.: Burning regimes for the finite-duration releases of fuel gases. In: Symposium (International) on Combustion, vol. 1, pp. 1549–1555 (1996). https://doi.org/10.1016/S0082-0784(96)80377-8

Makhviladze, G.M., Yakush, S.E.: Modelling of formation and combustion of accidentally released fuel clouds. Process Saf. Environ. Prot. **83**, 171–177 (2005). https://doi.org/10.1205/psep.04242

Makhviladze, G.M., Roberts, J.P., Yakush, S.E.: Modelling the fireballs from methane releases. Fire Saf. Sci. **5**, 213–224 (1997)

Makhviladze, G.M., Roberts, J.P., Yakush, S.E.: Fireball during combustion of hydrocarbon fueld releases II thermal radiation. Combust Explos Shock Waves **35**, 359–369 (1999b). https://doi.org/10.1007/BF02674465

Makhviladze, G., Roberts, J., Yakush, S.: Modelling and scaling of fireballs from single -and two-phase hydrocarbon releases. Fire Saf. Sci. **6**, 1125–1136 (2000). https://doi.org/10.3801/IAFSS.FSS.6-1125

Makhviladze, G.M., Roberts, J.P., Yakush, S.E.: Fireball during combustion of hydrocarbon fuel releases. I. Structure and lift dynamics. Combust. Explos. Shock Waves **35**, 219–229 (1999a). https://doi.org/10.1007/BF02674442.

Martinsen, W.E., Marx, J.D., By, P.: An improved model for the prediction of radiant heat from fireballs quest an improved model for the prediction of radiant heat from fireballs (1999)